Quantum simulation of Fermi-Hubbard models in semiconductor quantum-dot arrays

Tim Byrnes,[1,2] Na Young Kim,[3] Kenichiro Kusudo,[1] and Yoshihisa Yamamoto[1,3]
[1]*National Institute of Informatics, 2-1-2 Hitotsubashi, Chiyoda-ku, Tokyo 101-8430, Japan*
[2]*Institute of Industrial Science, University of Tokyo, 4-6-1 Komaba, Meguro-ku, Tokyo 153-8505, Japan*
[3]*E. L. Ginzton Laboratory, Stanford University, Stanford, California 94305, USA*
(Received 31 July 2008; published 25 August 2008)

We propose a device for studying the Fermi-Hubbard model with long-range Coulomb interactions using an array of coupled quantum dots defined in a semiconductor two-dimensional electron-gas system. Bands above the lowest energy band are used to form the Hubbard model, so that a high average electron density may be used to implement the device. We find that depending on the average electron density, the system is well described by a one- or two-band Hubbard model. Our device design enables the control of the ratio of the Coulomb interaction to the kinetic energy of the electrons independently to the filling of the quantum dots, such that a large portion of the Hubbard phase diagram may be probed. Estimates of the Hubbard parameters suggest that a metal-Mott insulator quantum phase transition and a *d*-wave superconducting phase should be observable using current technologies.

DOI: 10.1103/PhysRevB.78.075320 PACS number(s): 73.23.−b, 03.67.Lx, 71.10.Fd, 74.25.−q

I. INTRODUCTION

Along with quantum computers, quantum simulators promise to offer performance exceeding what is possible using only classical physics.[1] A quantum simulator is a device that is engineered to simulate a particular quantum many-body problem that is intractable on a classical computer. Several experiments and theoretical studies have indicated that such a device is possible to build.[2–10] Here we show that a similar device can be constructed for the fermionic Hubbard model using a semiconductor quantum-dot (QD) array system. One of the attractive features of using a semiconductor system over alternative approaches such as cold atoms in optical lattices[4,5] is that very low temperatures may be reached relative to the Fermi temperature. As we show in this paper, temperatures in the vicinity of $k_BT/t \approx 0.01$ (k_BT is the thermal energy, t is the Hubbard hopping amplitude) are accessible in semiconductor systems using dilution refrigerators. Another feature of the system is that due to the Coulomb interaction between the electrons, the form of the interaction is naturally long ranged. The two-dimensional Hubbard model is particularly interesting as it is one of the central models used to describe strongly-correlated phenomena such as metal-insulator transitions,[11] magnetism,[12] and high-temperature superconductivity.[13] Despite decades of intensive research, a complete solution remains unavailable due to difficulties in numerical and analytic methods.

II. THE DEVICE

The type of device we consider is an undoped GaAs/AlGaAs heterostructure, with a two-dimensional electron-gas system (2DEG) formed at the interface (Fig. 1). The 2DEG is formed by applying a positive voltage to a metallic top gate [the "global gate" (GG)].[14] Our choice of an undoped system, as opposed to a modulation doped system, is important for a clean realization of the Hubbard model so that impurities in the system are reduced to a minimum. In addition to the GG, a two-dimensional (2D) mesh gate (MG) is patterned over a large area (e.g., 30×30 μm^2) of the device. Applying a voltage to the MG induces an *in situ* tunable periodic lattice potential, such that an array of coupled QDs is created. The MG is separated by an electrically insulating layer from the GG, so that the average electron number in the QDs can be controlled independently of the inter-QD coupling.[14] The periodicity of the MG considered in this paper is $\lambda = 0.1$ μm, which is an experimentally achievable size using current lithography techniques. The use of a MG, as opposed to the surface acoustic wave (SAW) approach as discussed in Ref. 10, overcomes difficulties due to unavoidable sample heating induced by the SAW itself and complicated microwave engineering. The 2DEG is located at a shallow position relative to the surface in order to achieve sharp QD trapping potentials, as well as to reduce the overall Coulomb repulsion among electrons in a single QD via electrical screening from the metal gates. Without screening, the Coulomb interaction is typically larger than the kinetic energy $\frac{e^2}{4\pi\epsilon\lambda} > \frac{\hbar^2\pi^2}{2m^*\lambda^2}$ in our semiconductor system (e is the electron charge, $\epsilon \approx 13\epsilon_0$ is the permittivity, $m^* \approx 0.067 m_e$ is the effective electron mass in GaAs). The screening effect allows

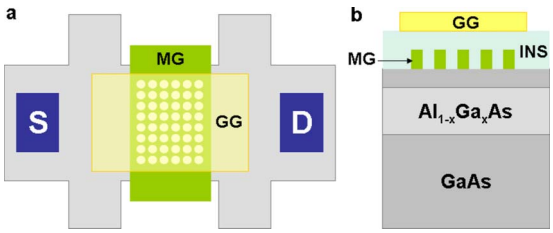

FIG. 1. (Color online) (a) A schematic top view of the proposed device. A two-dimensional Schottky mesh gate is patterned in the central region, and a top global gate is placed on top of the MG separated by an insulating layer such as Si_3N_4 (INS). Source (S) and drain (D) Ohmic contacts in the Hall bar mesa structure access the two-dimensional electron-gas system. (b) Cross-sectional view of the device. The 2DEG is formed at the interface between AlGaAs and GaAs by applying a voltage to the GG. The periodic potential is created by the 2D MG.

access to an interesting regime of the Hubbard model where quantum phase-transition (QPT) phenomena are expected to occur, with the Coulomb repulsion U and the nearest-neighbor hopping t being on the same order.

One of the key features of our device is that we consider average electron numbers beyond the occupation of the first band formed by the periodic potential. Typical high-mobility semiconductor samples have electron densities in the region of $\sim 10^{11}$ cm^{-2}, corresponding to ten electrons per QD for a periodicity of $\lambda = 0.1$ μm. Past studies[4,10] have assumed the occupation of only the lowest energy band of the imposed periodic potential. This corresponds to low electron densities where it is difficult to achieve high mobilities due to the presence of impurities. Low-density 2DEGs have also been experimentally observed to undergo a metal-insulator-like transition as a function of electron density.[15] In order not to mask the effects of the Hubbard model due to such low-density effects, it is advantageous to work in a high electron mobility regime where the system is in a metallic state.

III. THEORETICAL MODEL

A. Renormalized Coulomb interactions

Due to the presence of the electrons in the lower energy bands, the Coulomb interaction between two electrons in the higher energy bands will be renormalized by screening effects. In the standard procedure of obtaining an effective Hubbard model, one usually ignores the presence of the core electrons and considers only the outermost filled band of the periodic array.[12] In order to take into account the effect of the core electrons at a quantum-mechanical level, it is necessary to incorporate correlations between electrons in the outer orbitals and the core electrons. This can be done by the following procedure. First, model the 2DEG electrons in a periodic potential

$$V_M(\boldsymbol{x}) = V_0[\cos(2\pi x/\lambda) + \cos(2\pi y/\lambda)] \tag{1}$$

by a very general multi-Hubbard model

$$H = \sum_{\sigma \boldsymbol{n}\boldsymbol{n}' \boldsymbol{j}\boldsymbol{j}'} \mathcal{T}(\boldsymbol{n},\boldsymbol{n}',\boldsymbol{j},\boldsymbol{j}') c^\dagger_{\boldsymbol{j}\boldsymbol{n}\sigma} c_{\boldsymbol{j}'\boldsymbol{n}'\sigma} + \frac{1}{2} \sum_{\substack{\sigma\sigma' \\ \boldsymbol{n}_1\boldsymbol{n}_2\boldsymbol{n}_3\boldsymbol{n}_4 \\ \boldsymbol{j}_1\boldsymbol{j}_2\boldsymbol{j}_3\boldsymbol{j}_4}} \mathcal{U}(\boldsymbol{j}_1,\boldsymbol{j}_2,\boldsymbol{j}_3,\boldsymbol{j}_4,\boldsymbol{n}_1,\boldsymbol{n}_2,\boldsymbol{n}_3,\boldsymbol{n}_4) \times c^\dagger_{\boldsymbol{j}_1\boldsymbol{n}_1\sigma} c^\dagger_{\boldsymbol{j}_2\boldsymbol{n}_2\sigma'} c_{\boldsymbol{j}_3\boldsymbol{n}_3\sigma'} c_{\boldsymbol{j}_4\boldsymbol{n}_4\sigma}, \tag{2}$$

where $c_{\boldsymbol{j}\boldsymbol{n}\sigma}$ is the fermion annihilation operator associated with the site $\boldsymbol{j}=(j_x,j_y)$, band $\boldsymbol{n}=(n_x,n_y)$ (where $n_x,n_y \geq 1$), and spin σ. For each band $\boldsymbol{n}$ we may define a Wannier basis $w_{\boldsymbol{n}}(\boldsymbol{x})$, from which we may define the hopping

$$\mathcal{T}(\boldsymbol{n},\boldsymbol{n}',\boldsymbol{j},\boldsymbol{j}') = \int d^2x w^*_{\boldsymbol{n}}(\boldsymbol{x}-\boldsymbol{x}_{\boldsymbol{j}}) H_0(\boldsymbol{x}) w_{\boldsymbol{n}'}(\boldsymbol{x}-\boldsymbol{x}_{\boldsymbol{j}'}) \tag{3}$$

and Coulomb matrix elements,

$$\mathcal{U}(\boldsymbol{j}_1,\boldsymbol{j}_2,\boldsymbol{j}_3,\boldsymbol{j}_4,\boldsymbol{n}_1,\boldsymbol{n}_2,\boldsymbol{n}_3,\boldsymbol{n}_4) = \int d^2x \int d^2x' w^*_{\boldsymbol{n}_1}(\boldsymbol{x}'-\boldsymbol{x}_{\boldsymbol{j}_1}) w^*_{\boldsymbol{n}_2}(\boldsymbol{x}-\boldsymbol{x}_{\boldsymbol{j}_2}) U_C(\boldsymbol{x},\boldsymbol{x}') \times w_{\boldsymbol{n}_3}(\boldsymbol{x}-\boldsymbol{x}_{\boldsymbol{j}_3}) w_{\boldsymbol{n}_4}(\boldsymbol{x}'-\boldsymbol{x}_{\boldsymbol{j}_4}), \tag{4}$$

where the single electron Hamiltonian is $H_0(\boldsymbol{x}) = -\frac{\hbar^2}{2m^*}\nabla^2 + V_M(\boldsymbol{x})$. Due to the presence of the metal gates at the surface, we use a screened Coulomb interaction[10]

$$U_C(\boldsymbol{x},\boldsymbol{x}') = e^2 f_s(\boldsymbol{x},\boldsymbol{x}')/4\pi\epsilon|\boldsymbol{x}-\boldsymbol{x}'|, \tag{5}$$

where

$$f_s(\boldsymbol{x},\boldsymbol{x}') = 1 - |\boldsymbol{x}-\boldsymbol{x}'|/\sqrt{(x-x')^2+(y-y')^2+(z+z'+2d)^2}. \tag{6}$$

Now split the Hamiltonian (2) into two parts: one corresponding to "on-site" terms

$$H_{\text{on-site}} = \sum_{\sigma \boldsymbol{n} \boldsymbol{j}} \epsilon_{\boldsymbol{n}} c^\dagger_{\boldsymbol{j}\boldsymbol{n}\sigma} c_{\boldsymbol{j}\boldsymbol{n}\sigma} + \frac{1}{2} \sum_{\substack{\sigma\sigma' \boldsymbol{j} \\ \boldsymbol{n}_1\boldsymbol{n}_2\boldsymbol{n}_3\boldsymbol{n}_4}} \tilde{U}_{\boldsymbol{n}_1,\boldsymbol{n}_2,\boldsymbol{n}_3,\boldsymbol{n}_4} c^\dagger_{\boldsymbol{j}\boldsymbol{n}_1\sigma} c^\dagger_{\boldsymbol{j}\boldsymbol{n}_2\sigma'} c_{\boldsymbol{j}\boldsymbol{n}_3\sigma'} c_{\boldsymbol{j}\boldsymbol{n}_4\sigma}, \tag{7}$$

and the other corresponding to all the remaining terms $H_{\text{site-site}} \equiv H - H_{\text{on-site}}$. All terms in $H_{\text{site-site}}$ contain operators connecting two sites $\boldsymbol{j},\boldsymbol{j}'$ with $\boldsymbol{j}' \neq \boldsymbol{j}$. $H_{\text{on-site}}$ thus describes an array of independent QDs, while $H_{\text{site-site}}$ contains the interactions between them. In writing Eq. (7), we have used the identity

$$\mathcal{T}(\boldsymbol{n},\boldsymbol{n}',\boldsymbol{j},\boldsymbol{j}') = \frac{\delta_{\boldsymbol{n}\boldsymbol{n}'}\lambda^2}{4\pi^2} \int_{\boldsymbol{n}\text{th B.Z.}} d^2k E_{\boldsymbol{k}\boldsymbol{n}} e^{i\boldsymbol{k}\cdot(\boldsymbol{x}_{\boldsymbol{j}}-\boldsymbol{x}_{\boldsymbol{j}'})}, \tag{8}$$

where $E_{\boldsymbol{k}\boldsymbol{n}}$ is the energy dispersion of the $\boldsymbol{n}$th noninteracting band, and defined $\epsilon_{\boldsymbol{n}} \equiv \mathcal{T}(\boldsymbol{n},\boldsymbol{n},\boldsymbol{j},\boldsymbol{j})$ and $\tilde{U}_{\boldsymbol{n}_1,\boldsymbol{n}_2,\boldsymbol{n}_3,\boldsymbol{n}_4} = \mathcal{U}(\boldsymbol{j},\boldsymbol{j},\boldsymbol{j},\boldsymbol{j},\boldsymbol{n}_1,\boldsymbol{n}_2,\boldsymbol{n}_3,\boldsymbol{n}_4)$. $H_{\text{on-site}}$ has precisely the same form as the Hamiltonian of an array of isolated QDs.[16] The only difference here is that the single-particle basis is a Wannier basis, instead of the eigenstates of the confining potential. For this reason, we henceforth call the many-body system of electrons interacting via Hamiltonian (7) on a particular site a "Wannier quantum dot" (WQD). In the limit of very large barriers between the dots, $\epsilon_{\boldsymbol{n}}$ coincides exactly with the energy levels of an isolated QD.

B. Addition spectrum

In order to analyze the Hamiltonian (7), we have performed an exact diagonalization study for electron numbers up to $N=18$. Figure 2(a) shows the electron addition spectrum calculated according to[16]

$$A(N) = E_{N-1} + E_{N+1} - 2E_N, \tag{9}$$

where E_N is the ground-state energy of the N-particle Hamiltonian. We see a peak structure that reflects the shell structure of the WQD [shown in Fig. 2(b)], with peaks in $A(N)$

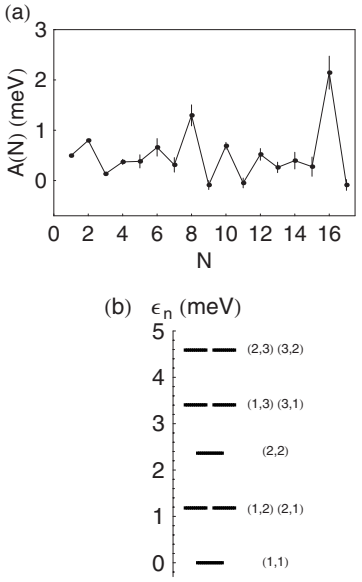

FIG. 2. (a) The addition energy $A(N)$ of a Wannier quantum dot with $\lambda=0.1$ μm, $V_0=0.28$ meV, and $d=10$ nm. Peaks occur at electron numbers corresponding to full and half filling of shells. (b) The single-particle energy spectrum $\epsilon_{\boldsymbol{n}}$ of a 2D WQD for each level $\boldsymbol{n}=(n_x,n_y)$ labeled.

occurring at the magic numbers of the WQD, i.e., electron numbers corresponding to completely filled shells. Unlike normal QDs, the shells are typically only doubly degenerate at most, originating from the x-y symmetry of the potential. We can thus expect that depending on the filling, we can approximate the system by either a one- or two-band Hubbard model. For electron numbers in the WQD corresponding to the doubly degenerate shells, we have verified that Hund's rule holds according to our numerical calculations, with ground states occurring for a total z component of spin $S_z=\pm 1$, rather than $S_z=0$ at half-filled shell fillings.

C. Effective Hubbard model

We may calculate the renormalized Coulomb interaction between electrons in the same band by using the diagonalized states of Eq. (7) to write down the effective Hubbard Hamiltonian. For fillings corresponding to a nondegenerate shell, make the state associations

$$|0\rangle_j \equiv |N_b,0,\boldsymbol{j}\rangle$$

$$|\uparrow\rangle_j \equiv |N_b+1,1/2,\boldsymbol{j}\rangle$$

$$|\downarrow\rangle_j \equiv |N_b+1,-1/2,\boldsymbol{j}\rangle$$

$$|\uparrow\downarrow\rangle_j \equiv |N_b+2,0,\boldsymbol{j}\rangle \tag{10}$$

for each site $\boldsymbol{j}$, where the eigenstates of Eq. (7) with energy E_{N,S_z} on a single site $\boldsymbol{j}$ are denoted $|N,S_z,\boldsymbol{j}\rangle$, and the total number of electrons in the lower energy "core" shells is called the base electron number N_b. In this paper, for simplicity we consider the single-band Hubbard approximation,

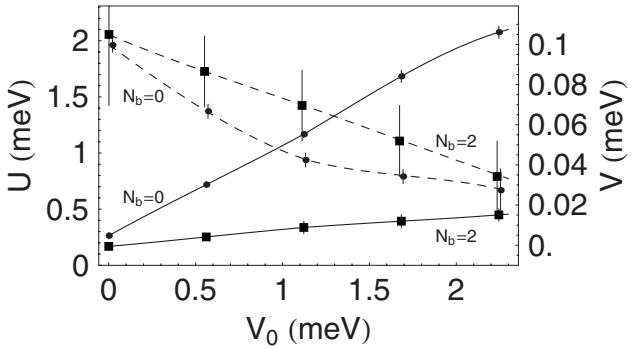

FIG. 3. The on-site Coulomb energy U (solid lines, left axis) for $N_b=0$ and $N_b=2$, and the nearest-neighbor Coulomb energy V (dashed lines, right axis) for $N_b=0$ and $N_b=2$ versus the periodic potential amplitude V_0 for $\lambda=0.1$ μm and $d=10$ nm. Error bars are estimated from the numerical covergence of the exact diagonalization.

although the generalization to the two-band case may be performed in a similar way.

Let us now introduce a particle number operator $n_{j\sigma}$ acting on the states $\mathcal{S}_j=\{|0\rangle_j,|\uparrow\rangle_j,|\downarrow\rangle_j,|\uparrow\downarrow\rangle_j\}$ with the properties

$$n_{j\sigma}|0\rangle_{j'}=0$$

$$n_{j\sigma}|\sigma'\rangle_{j'}=\delta_{jj'}\delta_{\sigma\sigma'}|\sigma'\rangle$$

$$n_{j\sigma}|\uparrow\downarrow\rangle_{j'}=\delta_{jj'}|\uparrow\downarrow\rangle. \tag{11}$$

In the space of $\mathcal{S}_j$, we may write down an effective Hamiltonian

$$H^{\text{eff}}_{\text{on-site}}=\sum_j\left(E_0+\sum_{\sigma=\pm 1/2}\mu_\sigma n_{j\sigma}+Un_{j\downarrow}n_{j\uparrow}\right), \tag{12}$$

where

$$E_0=E_{N_b,0}$$

$$\mu_\sigma=E_{N_b+1,\sigma}-E_{N_b,0}$$

$$U=E_{N_b+2,0}-\sum_{\sigma=\pm 1/2}E_{N_b+1,\sigma}+E_{N_b,0}. \tag{13}$$

The μ_σ is an effective chemical-potential term, while U is an effective Coulomb on-site repulsion energy. The expression for U has precisely the same form as that of the addition energy [Eq. (9)], which naturally arises since both are a measure of how much energy is required to overcome the Coulomb blockade in a QD. Figure 3 shows the on-site repulsion U as a function of the periodic potential amplitude for base electron fillings $N_b=0$ and 2, as well as the nearest-neighbor Coulomb integral using the standard single-band approximation. For $N_b=2$, we plot the average Coulomb energy between electron species in the two-band Hubbard model. We see that the periodic potential amplitude increases U and decreases V, in agreement with previous calculations.[10] The average Coulomb energy increases at a slower rate for $N_b=2$, due to the reduced localization for the higher energy electrons.

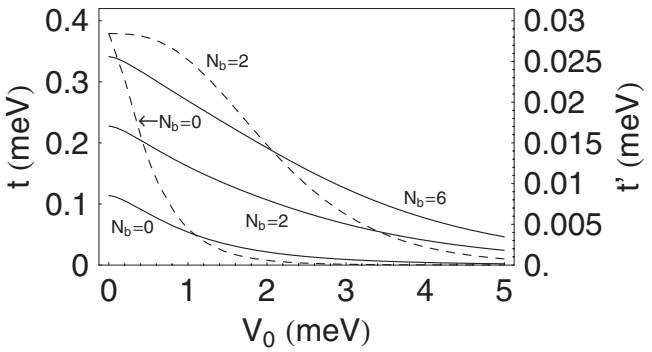

FIG. 4. The hopping t (solid lines, left axis) and the next-nearest-neighbor hopping t' (dashed lines, right axis) for $\lambda = 0.1$ μm versus the periodic potential amplitude V_0. The base electron numbers N_b for each t or t' are labeled.

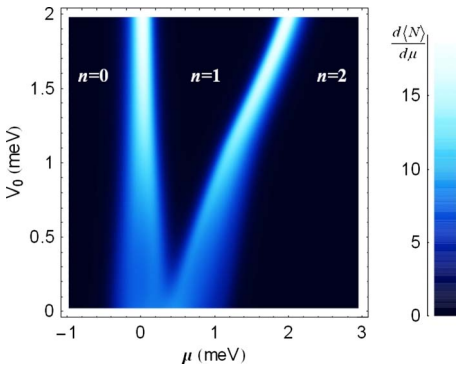

FIG. 5. (Color online) The electron addition spectrum $\frac{d\langle N\rangle}{d\mu}$, in the plane of the chemical potential μ and the potential amplitude V_0 at $T=1$ K and $\lambda=0.1$ μm. As μ is increased, electrons enter the Hubbard model at the densities n shown.

The hopping terms in the Hubbard Hamiltonian originate from transitions between the WQD eigenstates according to the intersite Hamiltonian $H_{\text{site-site}}$. They are calculated by transforming the hopping terms in $H_{\text{site-site}}$ into the truncated basis states $\mathcal{S}_j$. We find that the hopping is well approximated by the hopping integral of the band corresponding to the outermost shell of the noninteracting WQD. The nearest-neighbor hopping amplitudes for various base fillings N_b are plotted in Fig. 4. As the periodic potential is increased, the hopping is suppressed due to the increased strength of the barriers between the QDs. As the base filling N_b is increased, the hopping is enhanced due to the electrons occupying higher energy bands. On the other hand, we see from Fig. 2 that the large scale trend of the addition energy stays fairly constant with density. From Eq. (13), this suggests that the Coulomb energy U does not increase with density. Thus the overall effect of increasing the density is to shift the system into a more kinetic-energy dominated regime.

In order to ensure that a single or two-band approximation is valid, one must also consider whether interband transitions are suppressed sufficiently. For low temperatures $k_BT \ll \frac{\hbar^2}{2m^*\lambda^2}$, an approximate criterion is when there is no energy overlap between a given energy band and all other bands for the noninteracting band spectrum. A simple calculation reveals that the $N_b=0$ [or $\boldsymbol{n}=(1,1)$] band is separated from other bands in energy for $V_0>0.4$ meV, $N_b=2$ [or $\boldsymbol{n}=(1,2)$] is separated for $V_0>1.2$ meV, and the $N_b=6$ [or $\boldsymbol{n}=(2,2)$] is separated for $V_0>5.1$ meV. At potentials lower than these boundaries, the system cannot be described by a simple one- or two-band Hubbard model due to mixing of other bands with similar energies. However, since the dominant effect of increasing V_0 is to decrease the kinetic energy and increase the on-site Coulomb energy, we expect to be able to nevertheless tune the system from a kinetic energy dominated regime into a Coulomb energy dominated phase.

IV. MEASUREMENTS

By choosing a N_b with a small U/t and increasing the periodic potential V_0, we expect a metal-Mott insulator transition to occur in the system.[10,11] In our proposed device, such a transition may be identified by measuring the zero-bias differential conductance across the source and drain contacts. The conductance as a function of the chemical potential has been theoretically investigated in previous studies.[17] In the metallic state, the system will be conducting when the Fermi level lies within a band created by the applied periodic potential. In the Mott-insulating limit, the spectrum should reduce to that of a large array of isolated QDs. In Fig. 5, we calculate the addition spectrum by calculating the quantity $\frac{d\langle N\rangle}{d\mu}$ for various chemical potentials μ and potentials V_0, using the Hubbard parameters U, V, and t in Figs. 3 and 4 on a 2×3 lattice, according to the procedure given in Ref. 17. $\frac{d\langle N\rangle}{d\mu}$ is nonzero when electrons can flow into the system, thus reflects where the system is conducting. Figure 5 shows that as the chemical potential is raised, peaks in $\frac{d\langle N\rangle}{d\mu}$ are seen corresponding to the addition of a single electron to each site. In the system here, the electron number per site changes from $n=0$ to 1 to 2 as the chemical potential is raised. The origin of the chemical-potential difference between the peaks is a Coulomb blockade effect, which is the same as in a single quantum dot.[16] The system as a whole possesses a collective Coulomb blockade,[17] giving conductance peaks when the chemical potential overcomes the blockade energy. The "V"-shaped splitting of the peaks is characteristic of a Mott transition, with the region inside the V-shape being a Mott insulator. As the potential V_0 is decreased, the two branches of the V-shape merge into one, and the Mott-insulating region disappears. Below this potential the system may be described as a metal, while above this the system can be described as a Mott insulator.[17] In our calculations we have only considered a single Hubbard band, although in reality there are many bands as can be seen from Eq. (2). In general, each Hubbard band contributes a V-shape to the conductance diagram. Such oscillations in the conductances as a function of the chemical potential have been observed before, in works such as Refs. 18–20. However, a clear metal-insulator quantum phase transition has not been identified. Magnetoconductance measurements provide an independent check of a QPT between the metallic and Mott-insulating states. The phase-breaking length will reduce to a length comparable to the QD size in the case of a Mott-insulating QD array.[21]

In order that such QPT phenomena are not washed out due to temperature effects, we require the Hubbard param-

eters to be larger than the thermal energy $U,t \gg k_B T$.[22] Previous theoretical estimates have suggested that temperatures of $k_B T/t \approx 0.1$ are necessary to observe an antiferromagnetic (AF) phase, and $k_B T/t \approx 0.02$ for a d-wave superconducting (SC) phase.[4,23] According to Fig. 4 and taking into account the criterion for band separation discussed earlier, $k_B T/t \approx 0.01$ is readily reachable for $T \approx 10$ mK using current dilution refrigerator techniques. We thus expect that temperatures low enough to observe both the AF and SC phases are achievable with this system. The AF nature of the insulating phase can be determined from temperature-varying magnetic-susceptibility measurements.[24] Evidence of Cooper-pair formation may be obtained from the magnetocapacitance oscillation period, by observation of the Cooper-pair charge of $2e$ in the strongly coupled QD array.

V. SUMMARY AND CONCLUSIONS

We have proposed an experimentally viable quantum simulator for the one- and two-band Hubbard models using a semiconductor QD array device. For a given average electron number in the QDs, the low-energy physics may be described by an effective one- or two-band Hubbard model. Our scheme is easily generalized to different lattice geometries by adjusting the mesh gate design and voltage. Examining the region $U/t \gg 1$ produces an effective t-J or Heisenberg model, while spin models involving frustration may also be explored by fabricating a triangular lattice mesh gate. Another possibility is to introduce controlled disorder into the system by randomly varying the mesh dimensions in the lattice, and thereby producing a Hubbard-Anderson model.

ACKNOWLEDGMENTS

This work is supported by JST/SORST, NTT, the University of Tokyo, and the Special Coordination Funds for Promoting Science and Technology. We would like to thank M. Beasley, I. Fisher, M. Jura, M. Topinka, J. Berengut, and P. Recher for helpful discussions.

[1] R. P. Feynman, Int. J. Theor. Phys. **21**, 467 (1982).
[2] H. S. J. van der Zant, F. C. Fritschy, W. J. Elion, L. J. Geerligs, and J. E. Mooij, Phys. Rev. Lett. **69**, 2971 (1992).
[3] M. Greiner, O. Mandel, T. Esslinger, T. W. Hänsch, and I. Bloch, Nature (London) **415**, 39 (2002).
[4] W. Hofstetter, J. I. Cirac, P. Zoller, E. Demler, and M. D. Lukin, Phys. Rev. Lett. **89**, 220407 (2002).
[5] M. Köhl, H. Moritz, T. Stöferle, K. Günter, and T. Esslinger, Phys. Rev. Lett. **94**, 080403 (2005).
[6] A. Micheli, G. K. Brennen, and P. Zoller, Nat. Phys. **2**, 341 (2006).
[7] M. J. Hartmann, F. G. S. L. Brandão, and M. B. Plenio, Nat. Phys. **2**, 849 (2006).
[8] D. G. Angelakis, M. F. Santos, and S. Bose, Phys. Rev. A **76**, 031805(R) (2007).
[9] A. D. Greentree, C. Tahan, J. H. Cole, and L. C. L. Hollenberg, Nat. Phys. **2**, 856 (2006).
[10] T. Byrnes, P. Recher, N. Y. Kim, S. Utsunomiya, and Y. Yamamoto, Phys. Rev. Lett. **99**, 016405 (2007).
[11] M. Imada, A. Fujimori, and Y. Tokura, Rev. Mod. Phys. **70**, 1039 (1998).
[12] H. Tasaki, Prog. Theor. Phys. **99**, 489 (1998).
[13] T. Moriya and K. Ueda, Rep. Prog. Phys. **66**, 1299 (2003).
[14] R. L. Willett, M. J. Manfra, L. N. Pfeiffer, and K. W. West, Appl. Phys. Lett. **91**, 033510 (2007).
[15] S. Das Sarma and E. H. Hwang, Solid State Commun. **135**, 579 (2005).
[16] L. P. Kouwenhoven, D. G. Austing, and S. Tarucha, Rep. Prog. Phys. **64**, 701 (2001).
[17] C. A. Stafford and S. Das Sarma, Phys. Rev. Lett. **72**, 3590 (1994).
[18] K. Ismail, W. Chu, A. Yen, D. A. Antoniadis, and H. I. Smith, Appl. Phys. Lett. **54**, 460 (1989).
[19] L. P. Kouwenhoven, F. W. J. Hekking, B. J. van Wees, C. J. P. M. Harmans, C. E. Timmering, and C. T. Foxon, Phys. Rev. Lett. **65**, 361 (1990).
[20] R. J. Haug, J. M. Hong, and K. Y. Lee, Surf. Sci. **263**, 415 (1992).
[21] C.-T. Liang, C. G. Smith, J. T. Nicholls, R. J. F. Hughes, M. Pepper, J. E. F. Frost, D. A. Ritchie, M. P. Grimshaw, and G. A. C. Jones, Phys. Rev. B **49**, 8518 (1994).
[22] S. Sachdev, *Quantum Phase Transitions* (Cambridge University Press, Cambridge, England, 1999).
[23] T. A. Maier, M. Jarrell, T. C. Schulthess, P. R. C. Kent, and J. B. White, Phys. Rev. Lett. **95**, 237001 (2005).
[24] N. W. Ashcroft and N. D. Mermin, *Solid State Physics* (Cambridge University Press, Cambridge, England, 1976).